INTERNATIONAL JOURNAL FOR NUMERICAL METHODS IN FLUIDS, VOL. 24, 965–986 (1997)

SOME VALIDATION OF STANDARD, MODIFIED AND NON-LINEAR k–ε TURBULENCE MODELS

M. J. RABBITT[1]

[1]*Engineering Division, Nuclear Electric, Barnett Way, Barnwood, Gloucester GL4 7RS, U.K.*

SUMMARY

Standard, modified and non-linear k–ε turbulence models are validated against three axisymmetric flow problems—flow through a pipe expansion, flow through a pipe constriction and an impinging jet problem—to underpin knowledge about the solution quality obtained from two-equation turbulence models. The extended models improve the prediction of turbulence as a flow approaches a stagnation point and the non-linear model allows for the prediction of anisotropic turbulence. Significantly different values for the non-linear model coefficients are proposed in comparison with values found in the literature. Nevertheless, current turbulence models are still unable to accurately predict the spreading rate of shear layers. © 1997 by John Wiley & Sons, Ltd. Int. j. numer. methods fluids, 24: 965–986, 1997.

(No. of Figures: 21. No. of Tables: 0. No. of Refs: 11.)

KEY WORDS: turbulence models; k–ε; non-linear k–ε; finite element method; validation; FEAT

1. INTRODUCTION

Within Nuclear Electric the majority of turbulent flow calculations are carried out using the standard k–ε turbulence model, despite the availability of more accurate turbulence models such as Reynolds stress models. There are two main reasons why the Reynolds stress model is not currently used for applications. First, the cost of solution is generally an order of magnitude greater than an equivalent k–ε solution. Engineers do not currently have the time, nor is the computing power available, to conceive of using a Reynolds stress turbulence model to solve a large 3D turbulent flow problem. Secondly, the work required to make the model provide optimum-quality results is still large, basically because the effects of the pressure reflection term are so complicated. However, results from the standard k–ε model have limitations, particularly when the cross-sectional flow area changes, such as in flow through a diffuser or flow through a contraction. Consequently, there is a need to improve the predictions that come from the standard k–ε model. To this end, development has recently focused attention on extending the validity of two-equation turbulence models. The aim is to provide a wider range of problems for which a quality turbulent flow solution can be obtained than is currently available using the standard k–ε model, but at an equivalent cost.

The success of the work depends on the availability of quality experiments for validation. The validation has so far concentrated on axisymmetric problems as these are considerably cheaper than three-dimensional problems and hence a significant range of modelling options can be tried out owing to a quick turnover of results. This paper describes three such problems: flow in a pipe expansion,

CCC 0271–2091/97/100965–22$17.50 *Received March 1996*

flow through a pipe constriction and an impinging jet problem. All these problems have an associated quality experimental database of results.[1–3] Nuclear Electric's FEAT[4] has been used for the calculations.

The behaviour of two turbulence models, which are both extensions of the standard k–ε model, is investigated for these axisymmetric validation problems and compared with results from the standard model and measurements. The first model, called the modified model, modifies the source terms in the equations for the turbulence variables with the aim of preventing the excessive generation of turbulence at a stagnation point. The second model, called the non-linear model, provides a mechanism for anisotropy of the normal stresses; the modelling demands aimed for in this work are first to improve the prediction of turbulence generation near a stagnation point and secondly to provide a mechanism for providing anisotropy of the turbulent velocity correlations with consequent improved results. The results from the comparisons can be used to determine, for example, whether the model constants used in the standard k–ε model should be retuned to improve results or whether any enhancement in quality from the extended models is sufficient instead.

The overall aim of research in turbulence modelling nowadays is not to provide a general turbulence model. Instead, the aim is to provide the engineer with guidance about problems for which particular turbulence models can or cannot be used. The aim of this paper is to provide indications about the performance of the two-equation turbulence models considered for three axisymmetric validation problems.

2. FEAT

FEAT stands for Finite Element Analysis Toolkit.[4] This section briefly clarifies the important modelling and facilities used to solve the turbulent forced convection flow problems that are described in this paper.

2.1. Cost versus accuracy

In FEAT the field variables (e.g. fluid velocity components, turbulence variables, temperature, etc.) are modelled using quadratic basis functions. The method used ensures that solutions are fourth-order-accurate. The cost of obtaining solutions to a given level of accuracy is significantly lower with FEAT than with current flow codes based on traditional finite difference techniques.[5] This latter point is crucial to the reason why FEAT can be successfully deployed to obtain accurate solutions on relatively coarse meshes.

2.2. Two-equation turbulence modelling

The method of calculation for the turbulence variables is through the solution of transport equations for q and f, where $k = q^2$ and $\varepsilon = fq^2$. This formulation allows solutions to be obtained that are fourth-order- accurate even in the turbulence variables.[4,6]

There are several possible options available to model near-wall flows. In principle, owing to improved modelling accuracy, the best option currently available is to solve low-Reynolds-number versions of the q and f equations (without the terms that ensure equivalence with the k–ε equations) near the wall and to solve the k–ε model in the turbulent core; this model is equivalent to the currently fashionable k–ω model. However, current experience with the model shows that the process is generally too expensive for 3D problems, as many elements are required near walls. The reason for this is that f (or ω) varies like $1/x$ within the log layer as a wall is approached, which is quite a steep variation that needs resolving. There is, however, some room for improvement in this area of research; a low-Reynolds- number model that involves the variable $1/f$ (or $1/\omega$) should reduce the

cost of solution. This has got much better properties than the k–ω model, because the variation near a wall is linear within the log layer and consequently much cheaper to resolve. Since, however, this improved option is currently not available, a wall-function-type approach is adopted for the calculations described in this paper.

2.2.1. Wall region of turbulent flows. The wall region is spanned with a single element in the direction normal to the wall by making certain modifications to the transport equations in that region. The modelling in the wall elements is called wall function modelling. The aim of the method is to model the effect of the wall on the rest of the flow whilst modelling the near-wall flow as well as possible in one element's width. A complete description of the method used in FEAT is given elsewhere[4] and a basic outline is provided here. The basic assumptions are that there is no flux of q from the wall into the turbulent flow, the shear stress is constant normal to the wall and the length scale follows the correlation

$$l = C_\mu^{1/4} \kappa y,$$

where y is the distance from the wall. With these assumptions the sources and sinks in the q equation are amenable to averaging over the near-wall region. Generating a depth-averaged f equation is difficult, however, since the conservation of f depends on a balance of very large terms. FEAT therefore uses a synthetic f equation near the wall which reproduces the length scale correlation in equilibrium boundary layers but also takes account of transport effects when conditions deviate from this.

It is not the intention of this paper, however, to investigate different types of wall modelling. To eliminate any sensitivity of the results to wall modelling, the same wall functions are prescribed for all the two-equation turbulence models used in the calculations.

2.3. Turbulent flow steady state solvers in FEAT

The frontal linear equation solver method is used in conjunction with the Newton–Raphson iteration technique to solve non-linear problems. To solve a turbulent flow problem, 'turbulent cycling' is carried out. Initial very simple distributions of the turbulence variables are provided by the user. These are used to carry out one Newton–Raphson iteration of the Navier–Stokes equations. The equations for the turbulence variables (q and f) are then solved, decoupled, until they converge, at which point the new values are relaxed with values prior to their update, the relaxation parameter being calculated from the history of previous changes. The process is continued until overall convergence is achieved, which normally means that all variables change by less than 0·3 per cent at all nodes between cycles. The solution process generally takes between 10 and 20 cycles to converge.

2.4. Quantifying mesh errors

The finite element methodology used by FEAT naturally produces mesh oscillations. Mesh oscillations occur because the solutions at corner and mid- side nodes are only loosely coupled, the magnitude of the coupling being proportional to the lack of mesh resolution. Thus, where the mesh resolves the flow well, the coupling is good and mesh oscillations are small, but where the mesh resolution is poor, the coupling is low and significant mesh oscillations occur. The net effect is that the leading-order error is an oscillation about the correct solution.

The size of any mesh oscillations can be used to judge where the mesh needs refining and can further be used to estimate the accuracy of the solution. FEAT has a facility for estimating the absolute errors given the variation of a quadratic variable on a finite element mesh. This is very

useful, as it is not necessary to perform a mesh refinement study to quantify errors. This ultimately saves a considerable amount of time and money.

2.4.1. Basic approach. In a k–ε forced convection solution the turbulence variables contribute to mesh error as well as the velocity. To obtain a measure of the error at every point, therefore, the contributions from all variables are incorporated in quadrature at every point, i.e.

$$error = [(qerr/q)^2 + (ferr/f)^2 + (sperr/speed)^2]^{0{\cdot}5}, \tag{1}$$

where *sperr* combines contributions to mesh error from the velocity components.

An indication of the overall mesh error in wall shear stress, for example, can be obtained by considering errors in elements next to walls.

The mesh errors at any point will be influenced by what happens within the rest of the mesh, as errors are both convected and diffused, and this is not incorporated in the method described. However, the method does indicate where the errors are introduced because of inferior resolution.

3. NON-LINEAR TURBULENCE MODEL

3.1. Theory

The reasoning behind the non-linear k–ε model is excellently explained elsewhere.[7] The non-linear model used in this paper is an extended version.[8]

The turbulent velocity cross-correlations are specified as

$$\begin{aligned}\overline{(u_i'u_j')} = {} & \tfrac{2}{3}k\delta_{ij} - \nu_t S_{ij} + c_1\frac{\nu_t}{f}(S_{ik}S_{kj} - \tfrac{1}{3}S_{kl}S_{kl}\delta_{ij}) \\ & + c_2\frac{\nu_t}{f}(\Omega_{ik}S_{kj} + \Omega_{kj}S_{ki}) + c_3\frac{\nu_t}{f}(\Omega_{ik}\Omega_{jk} - \tfrac{1}{3}\Omega_{kl}\Omega_{kl}\delta_{ij}) \\ & + c_4\frac{\nu_t}{f^2}(S_{ki}\Omega_{lj} + S_{kj}\Omega_{li} - \tfrac{2}{3}S_{km}\Omega_{lm}\delta_{ij})S_{kl} + c_5\frac{\nu_t}{f^2}S_{ij}S_{kl}S_{kl} + c_6\frac{\nu_t}{f^2}S_{ij}\Omega_{kl}\Omega_{kl},\end{aligned} \tag{2}$$

where $\nu_t = ql$, $k = q^2$, $l = C_\mu q/f$ and

$$S_{ij} = \frac{\partial u_i}{\partial x_j} + \frac{\partial u_j}{\partial x_i}, \qquad \Omega_{ij} = \frac{\partial u_i}{\partial x_j} - \frac{\partial u_j}{\partial x_i}.$$

S_{ij} is a symmetric tensor and Ω_{ij} is an antisymmetric tensor, i.e. $\Omega_{ij} = -\Omega_{ji}$. In axisymmetry, $S_{33} = 2u_r/r$. Full realizability (i.e. $\overline{(u_1'u_1')}$, $\overline{(u_2'u_2')}$ and $\overline{(u_3'u_3')}$ all greater than zero) is not guaranteed by this model.

$c_1 = -0{\cdot}1$, $c_2 = 0{\cdot}1$, $c_3 = 0{\cdot}26$, $c_4 = -1{\cdot}0$, $c_5 = -0{\cdot}1$ and $c_6 = 0{\cdot}1$ are the proposed default values,[8] although no justification is given in Reference 8.

3.1.1. Momentum equations. The momentum equations take the form

$$\rho u_j\frac{\partial u_i}{\partial x_j} = -\frac{\partial p}{\partial x_i} + \frac{\partial \mu S_{ij}}{\partial x_j} + \frac{\partial \sigma_{ij}}{\partial x_j}, \tag{3}$$

where for a general turbulent flow the imposed symmetric stress tensor is given by

$$\sigma_{ij} = -\rho\overline{(u_i'u_j')}. \tag{4}$$

For the non-linear k–ε model, $\overline{(u_i'u_j')}$ are defined by (2). During turbulent cycling, the Reynolds stresses (4) are relaxed in the same way as the q and f variables.

3.1.2. Turbulence, q and f equations. The turbulence generation term in the k equation takes the form

$$SOURCE_k = -\overline{(u_i' u_j')}\frac{\partial u_i}{\partial x_j} \tag{5}$$

in Cartesian geometry and

$$SOURCE_k = -\overline{(u_i' u_j')}\frac{\partial u_i}{\partial x_j} + 2\overline{(u_3' u_3')}\frac{u_r}{r} \tag{6}$$

in axisymmetry. The source in the q equation, $SOURCE_q$, is $SOURCE_k$ divided by q. For the source in the f equation, $SOURCE_f$, $SOURCE_k$ as defined above is divided by ql and multiplied by $C_\mu C_{1f}$.

The source terms in the q and f equations defined by the above expressions are smoothed via element averaging before inclusion in the q and f equations.

3.1.3. Notes about 2D flows. $\overline{(u_1' u_1')} = \overline{(u_2' u_2')}$ in the terms involving c_1, c_2 (which are zero), c_3 and c_4 (which again are zero), i.e. the only anisotropic contributions come from the terms involving the coefficients c_5 and c_6. Consequently, in 2D flows (but not axisymmetric) the turbulence model anisotropy is totally dependent on these two terms and the size of the coefficients. Without the terms involving c_5 and c_6, the solutions obtained are similar to standard k–ε solutions, as the additional stress tensor contributions are isotropic.

3.1.4. Notes about axisymmetric flows. The following comments are only true for non-swirling axisymmetric flows.

1. The c_2 term does not contribute to the normal stresses and therefore does not provide a mechanism for anisotropy of the turbulence. The term does, however, provide a contribution to the shear stress.
2. The c_3 term provides $\overline{(u_1' u_1')} = \overline{(u_2' u_2')}$ and $\overline{(u_1' u_2')} = 0$. This is therefore modelling isotropic turbulence in axisymmetry. $c_3 = 0{\cdot}26$ is the proposed default value,[8] but no evidence is presented to say how this coefficient was found.
3. Although the velocity correlations are affected by the c_4 term, the term makes no direct contribution to the sources in the q equation.
4. Anisotropy is modelled by the c_1, c_5 and c_6 terms.
5. Mechanisms for the transfer of the mean flow energy into both normal and shear stresses are provided by the c_1, c_2, c_5 and c_6 terms.

4. MODIFIED TURBULENCE MODEL

4.1. Theory

For the modified k–ε model the source terms in the two equations are modified. The source terms change from

$$SOURCE_q = \frac{1}{2}S_{ij}S_{ij}, \qquad SOURCE_f = \frac{C_\mu C_{1f}}{2}S_{ij}S_{ij} \tag{7}$$

to

$$SOURCE_q = \frac{1}{\sqrt{2}}(S_{ij}S_{ij}\Omega_{ij}\Omega_{ij})^{1/2}, \qquad SOURCE_f = \frac{C_\mu C_{1f}}{\sqrt{2}}(S_{ij}S_{ij}\Omega_{ij}\Omega_{ij})^{1/2} \tag{8}$$

5. VALIDATION PROBLEMS

The axisymmetric problems of flow in a pipe expansion, flow through a pipe constriction and an impinging jet were used to validate the models by comparing with the experimental data available.[1–3] The validation has concentrated primarily on the prediction of turbulence structure and important parameters such as the pressure drop through the pipe constriction. This is in contrast with a lot of validation work in the literature that has limited itself solely to the prediction of eddy lengths. Although some information can be obtained by obtaining eddy lengths, none is obtained about the main features of interest to an engineer, such as the prediction of pressure drop or turbulence (e.g. heat transfer). These are far more important to validate.

5.1. Pipe expansion problem

5.1.1. Description of problem and standard model results. This problem is fully described elsewhere;[1] the reader is referred to Figure 1 for a specification of the problem. The mesh used for the calculations had 2052 elements and is shown in Figure 2. The specified inlet profiles for the two velocity components, turbulence energy q and turbulent length scale are shown in Figure 3. Figure 4 shows contours of streamfunction, q and length scale obtained from the standard k–ε turbulence model.

Figure 5 shows contours of mesh error from the standard k–ε solution. The process outlined above for indicating mesh error gave an estimate for the root mean square mesh error in the wall elements of about 1·7 per cent, dominated by the values in the vicinity of the expansion. The overall errors in the solution are acceptably small. The k–ε solution obtained is within the consensus provided.[9]

For the non-linear model results described, the only non-zero terms used were those involving the c_1 and c_2 terms; c_1 was set to $-0{\cdot}1$ and c_2 was set to $0{\cdot}1$. The other coefficients were set to zero.

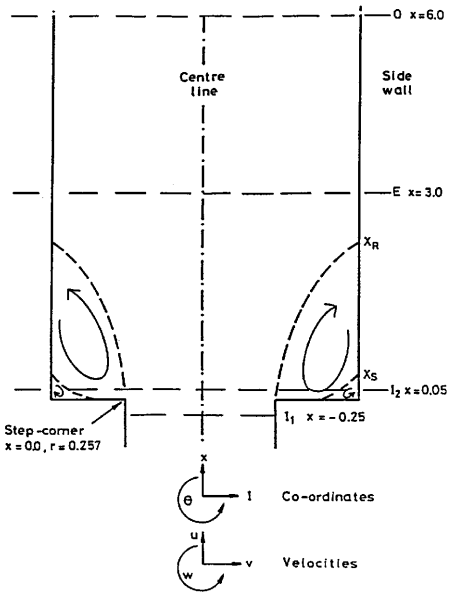

Figure 1. Specification of pipe expansion problem

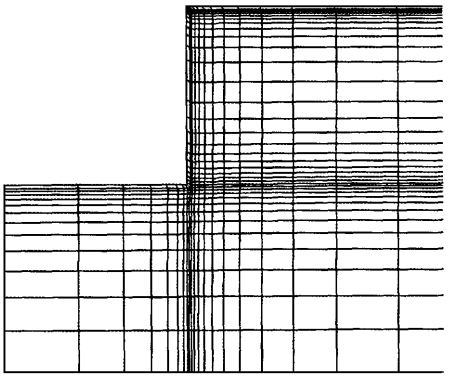

Figure 2. Finite element mesh used for pipe expansion problem in vicinity of step edge

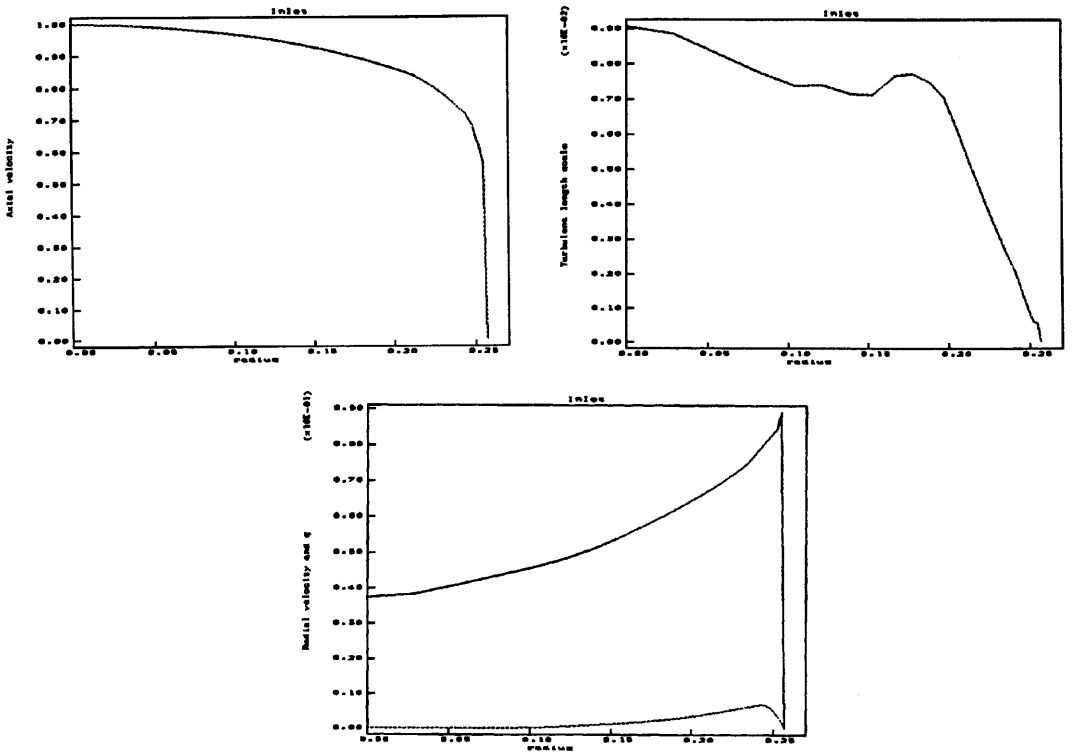

Figure 3. Inlet profiles of axial and radial velocity components, turbulence energy q and turbulent length scale for pipe expansion problem

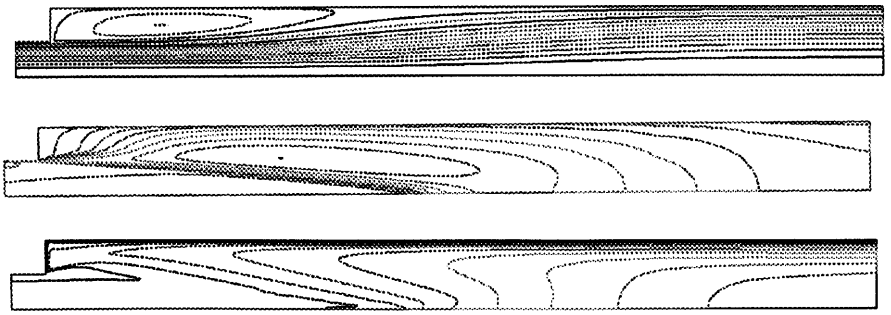

Figure 4. Contours of (from top) streamfunction, q and length scale for pipe expansion problem

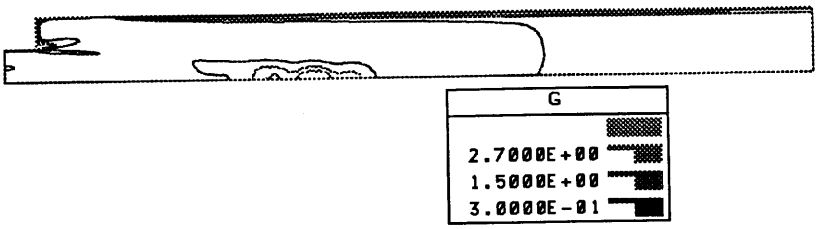

Figure 5. Contours of percentage mesh error

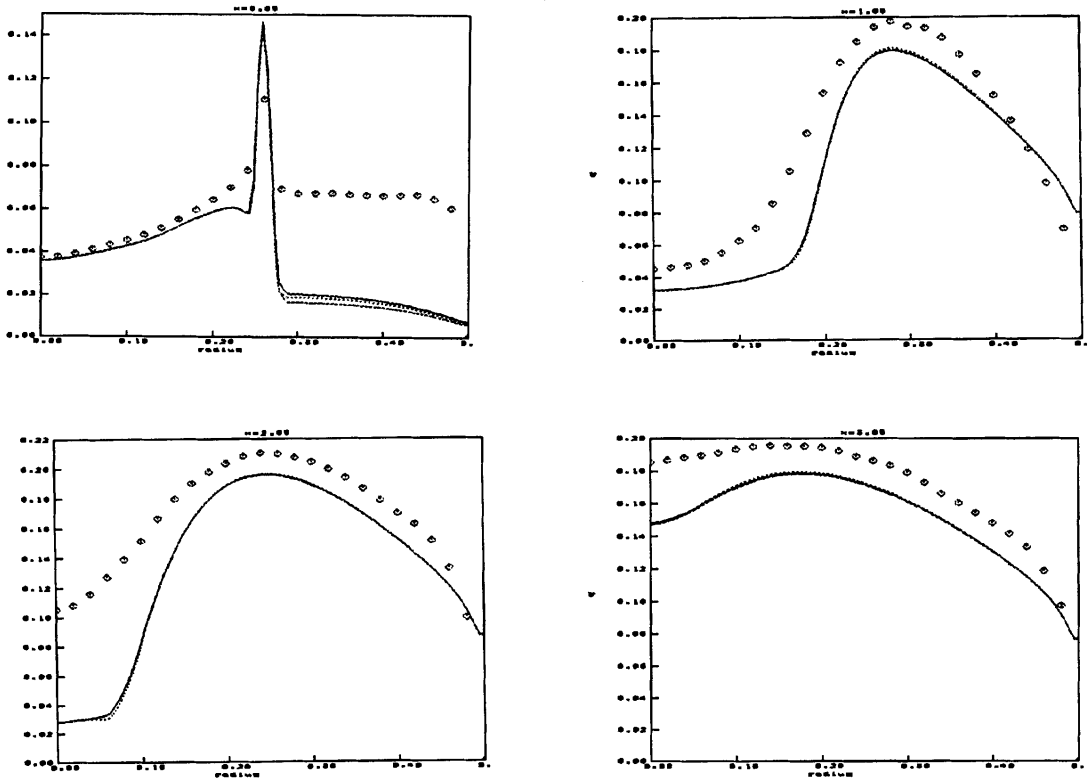

Figure 6. Radial profiles of q at axial locations $x = 0{\cdot}05$, $1{\cdot}05$, $2{\cdot}05$ and $3{\cdot}05$: symbols, experimental measurements; lines, results from standard, modified and non-linear models

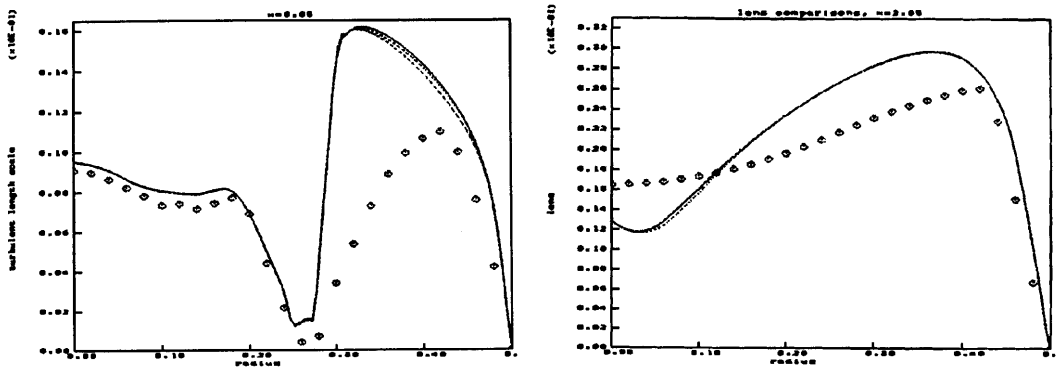

Figure 7. Radial profiles of length scale at axial locations $x = 0{\cdot}05$ and $2{\cdot}05$

5.1.2. Results and comparison with experiment. Figure 6 shows the comparison between predicted and measured turbulence energy profiles for the standard, modified and non-linear models at various axial locations. The results produced by the different turbulence models are almost indistinguishable from each other. Figure 7 shows the comparison between predicted and measured length scale profiles for the three models at $x = 0{\cdot}05$ and $2{\cdot}05$. Again the predictions are very similar for all the models. Radially outboard of the expansion the length scales are consistently predicted to be too large in comparison with the experimental values. The extended models therefore provide no improvement in prediction for the pipe expansion problem.

Whilst there is qualitative agreement, the detail of the flow is incorrect. The most significant factor is that the calculated spreading rate of the shear layer is too great. There is qualitative agreement in the axial development of k from the step edge, Figure 8, but a significant difference in the centreline development, Figure 9. The delay in growth of k and decay of axial velocity along the centreline are consistent with each other. For the record the annular shear layer reaches the wall at $x = 2{\cdot}53$ (where the wall shear stress is zero) in comparison with the experimental value of $2{\cdot}3$.

The non-linear model does not predict significantly anisotropic turbulence for this flow (as $\overline{(u_1'u_1')} \sim \overline{(u_2'u_2')}$). Figure 10 shows contours of $\overline{(u_1'u_1')}$ (which is very similar to $\overline{(u_2'u_2')}$) and $\overline{(u_3'u_3')}$, both in comparison with the experiment. Whereas the experiment shows anisotropy of $\overline{(u_1'u_1')}$ and $\overline{(u_2'u_2')}$ within the shear layer, the predictions do not. The peak values of $\overline{(u_1'u_1')}$ within the shear layer

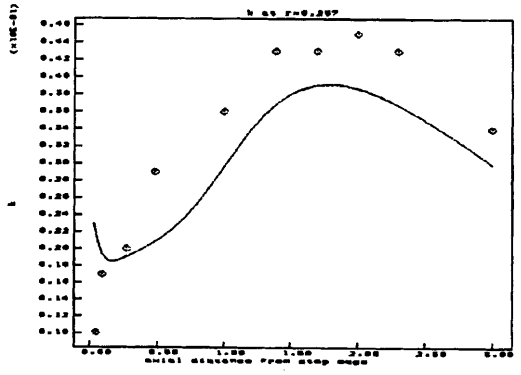

Figure 8. Axial profile of turbulence energy k at $r = 0{\cdot}257$ from step edge

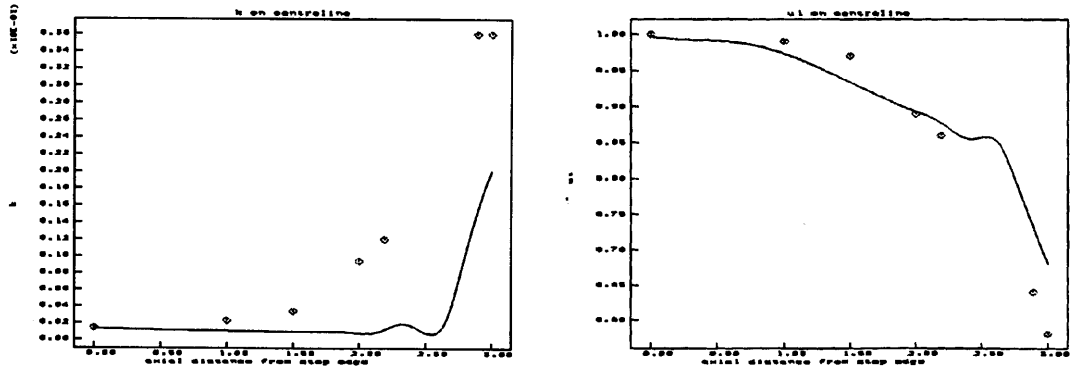

Figure 9. Axial profiles of turbulence energy k and axial velocity on centreline

are underpredicted by about a factor of two. Figure 10 also shows contours of $\overline{(u_1' u_2')}$, which is in good agreement with the experiment.

The reason why the agreement between measured and predicted turbulence levels is not very good on the radial profile at $x = 0{\cdot}05$ within the recirculation region is that the u_3' component of turbulence was measured to be significantly larger (a maximum of 2 per cent of the bulk flow speed) than the other two components. Within the recirculation region both $\overline{(u_1' u_1')}$ and $\overline{(u_2' u_2')}$ are suppressed in the experiment but $\overline{(u_3' u_3')}$ is not, whereas the turbulence models predict suppression of $\overline{(u_3' u_3')}$ as well. This would seem to be a consequence of a one-length-scale turbulence model; the small monolength scale causes the suppression of all normal stresses within the recirculation, whereas in reality the $\overline{(u_3' u_3')}^2$ component is affected by the relatively large circumferential length scale. There is a clear indication in the experiment of the presence of more than one length scale, namely one within the recirculation region and one within the shear layer, from consideration of the energy spectra.[10] This is therefore a likely explanation for the discrepancy within the recirculation and also within the centreline edge of the shear layer. Replacing the measured turbulence energy levels in the corner by the contributions from the u_1' and u_2' components only, the predictions given by the k–ε models are about right.

Using values of c_1 and c_2 which were -1 times the suggested default values (i.e. $c_1 = 0{\cdot}1$, $c_2 = -0{\cdot}1$) gave results which were very similar to those already presented, as these two terms nearly cancel for this flow (i.e. $\Omega_{ij} \sim S_{ij}$). It was also not possible to significantly change turbulence fields by altering the value of c_6.

In conclusion, the non-linear, modified and standard k–ε models provide very similar solutions for the pipe expansion problem and no advantage is gained by using the extended models. All the solutions give acceptable agreement for the gross features in the flow when compared with the measurements, apart from within the recirculation region, where turbulence levels are significantly underpredicted, and near the centreline edge of the shear layer, owing to the poor prediction of the spreading rate of the shear layer. Both of these are probably a consequence of using a one-length scale- turbulence model, which may be inadequate in these regions.

5.2. Pipe constriction problem

5.2.1. Description of problem and standard model results. A description of the problem is given elsewhere.[2] The inside diameter of the pipe upstream from the constriction is 0·0508 m. The total

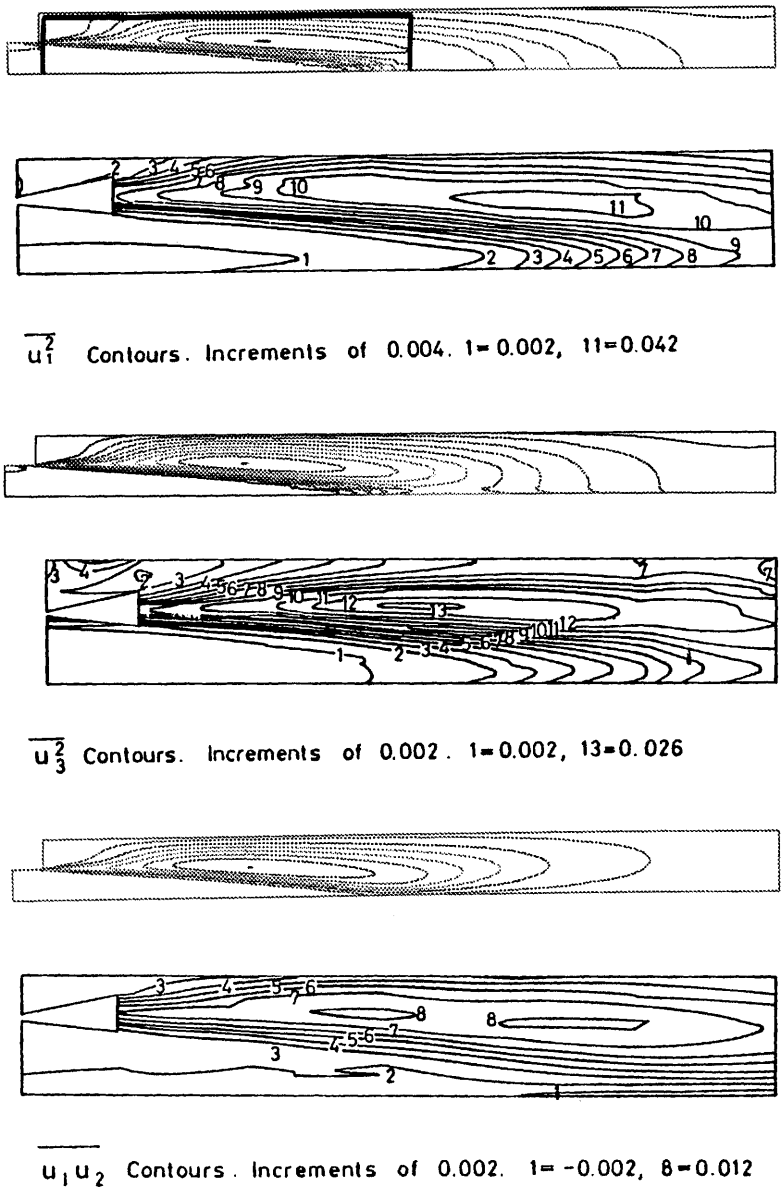

Figure 10. Contours of $\overline{(u_1' u_1')}$ (largest contour value 0·022), $\overline{(u_3' u_3')}$ (largest contour value 0·026) and $\overline{(u_1' u_2')}$ (largest contour value 0·012) along with experimental comparisons. The top contour plot also indicates the window relevant to the experimental comparisons shown

distance between the start and finish of the constriction is $2 \times 0{\cdot}0508$ m. The constriction geometry is given by the equation

$$R_0(Z) = r_0(Z)/a_0 = \begin{cases} 1 - \frac{1}{4}[1 + \cos(\frac{1}{2}\pi Z)], & -2 \leqslant Z \leqslant 2, \\ 1, & |Z| > 2, \end{cases} \tag{9}$$

where a_0 is the unoccluded tube radius (0·0254 m) and R and Z are the dimensionless radial and axial variables respectively. A Reynolds number of 15,000 was specified. Upstream of the constriction,

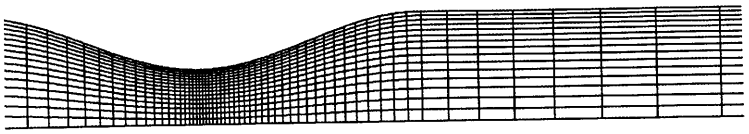

Figure 11. Finite element mesh for pipe constriction problem in vicinity of constriction

sufficient mesh was provided to produce a fully developed flow at the entrance to the constriction, as specified in the experiment. Figure 11 shows the mesh used for the calculations in the vicinity of the constriction.

Figure 12 shows contours of streamfunction, q and length scale for the standard model. The standard model erroneously predicts turbulence generation within the constriction upstream of the throat.

Figure 13 shows contours of mesh error. The process outlined above for indicating mesh errors gave a root mean square error of 1·1 per cent in the elements next to the walls within the constriction (which is where the mesh errors are largest). The mesh errors are therefore acceptably small.

5.2.2. Results and comparison with experiment. For all the profiles shown for this problem, the turbulence speed and axial velocity are both scaled by the bulk velocity upstream of the constriction.

Figure 14 shows the comparison of predicted and measured profiles of q at various axial locations along the pipe, Figure 15 shows the comparison of predicted and measured profiles of axial velocity and Figure 16 shows the static pressure variation along the pipe wall for all the models. Results from the two extended models are described separately.

5.2.3. Modified model. The results obtained from the modified model are an improvement over those from the standard k–ε model, particularly upstream of the throat. Figure 14 shows that turbulence is not erroneously generated upstream of the constriction. Downstream of the constriction the results are similar to the standard k–ε model.

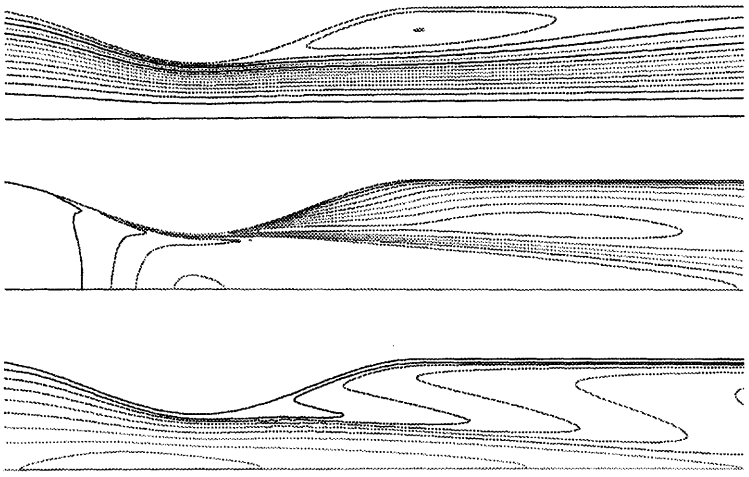

Figure 12. Contours of (from top) streamfunction, q and length scale for pipe constriction problem

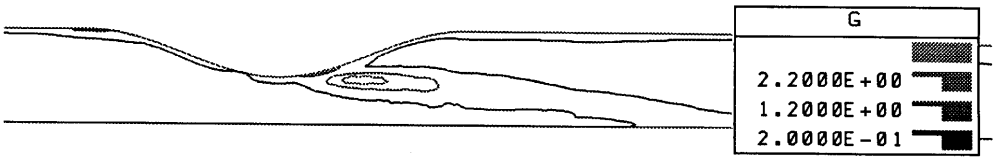

Figure 13. Contours of percentage mesh error

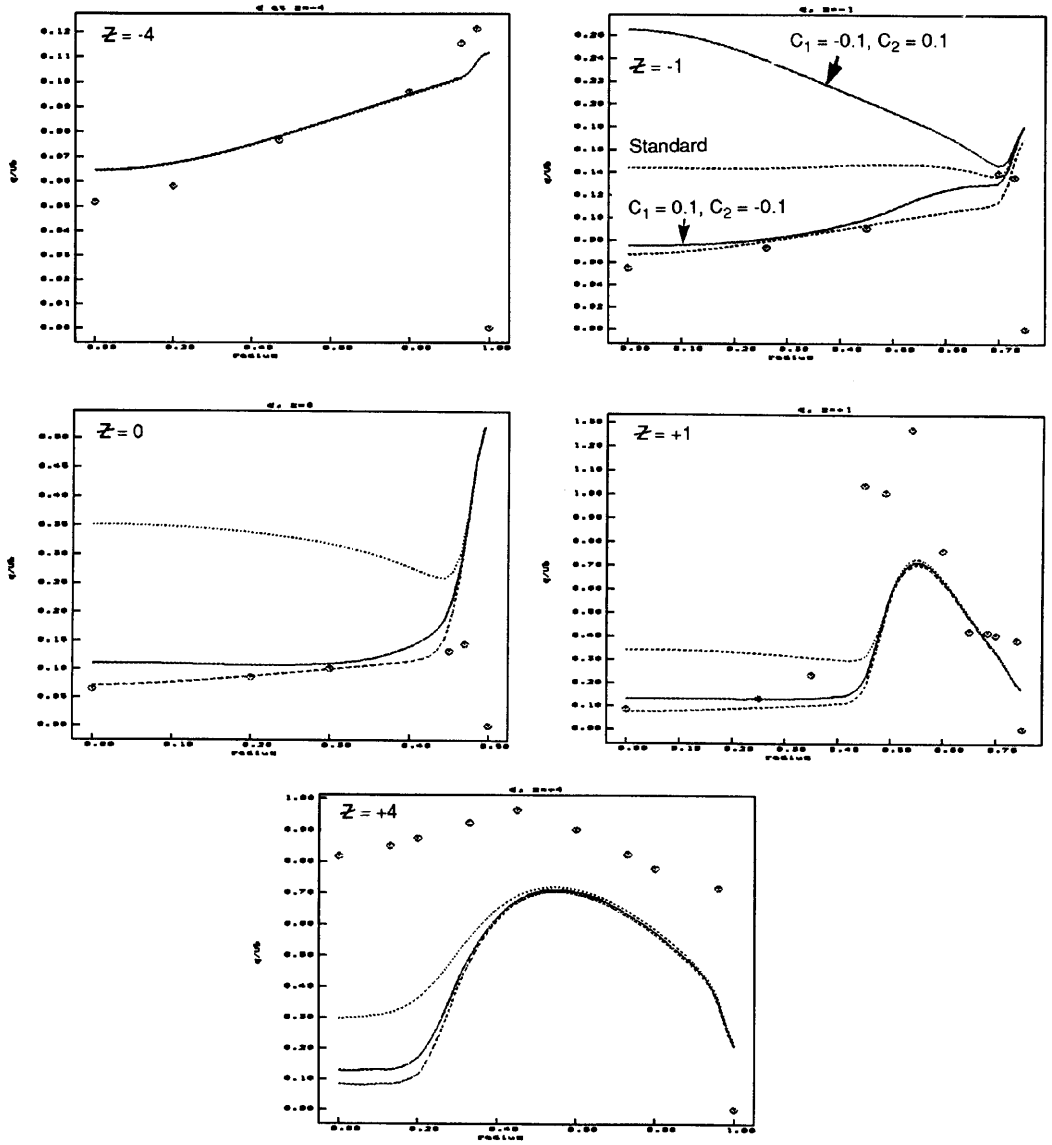

Figure 14. Radial profiles of turbulence speed q/U_b at axial locations $Z = -4, -1, 0, 1$ and 4 for pipe constriction problem: symbols, experimental measurements; dotted lines, standard model; broken lines, modified model; full lines, non-linear model

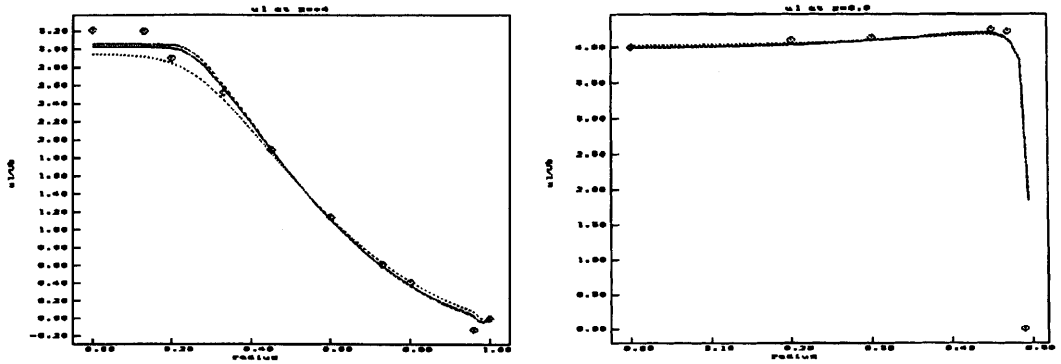

Figure 15. Radial profiles of axial velocity u_1/U_b axial locations $Z=0$ and 4 for pipe constriction problem: symbols, experimental measurements; dotted lines, standard model; broken lines, modified model; full lines, non-linear model

5.2.4. Non-linear model. For the terms involving c_1 and c_2, two cases have been considered, first with c_1 and c_2 set to the default values of $-0{\cdot}1$ and $0{\cdot}1$ and secondly with them set to $0{\cdot}1$ and $-0{\cdot}1$ (i.e. -1 times the default values). Some calculations were also carried out separately incorporating the c_3, c_5 and c_6 terms.

The advantage that the non-linear k–ε model has is that anisotropy of turbulence is possible and for this problem there is significant anisotropy downstream of the throat, but still within the constriction, and also slightly upstream of the throat. Anisotropy is predicted by the non-linear k–ε model slightly upstream of the throat, but downstream of the throat the predicted anisotropy is small. In comparison with measurements, therefore, the prediction of the position of anisotropy is good upstream but poor downstream of the throat.

With c_1 and c_2 set to their default values, the results obtained are significantly worse than those from the standard k–ε model upstream of the throat, as shown in Figure 14. Even more erroneous turbulence is generated upstream of the throat in comparison with the standard k–ε model. With c_1 and c_2 set to -1 times their default values, however, the prediction upstream of the throat is in good agreement with the measurements, since no erroneous turbulence is generated, as shown in Figure 14. Downstream of the constriction, agreement is similar to the standard k–ε model results for both cases. It is clear, therefore, that the c_1 term is directly responsible for suppressing the erroneous turbulence

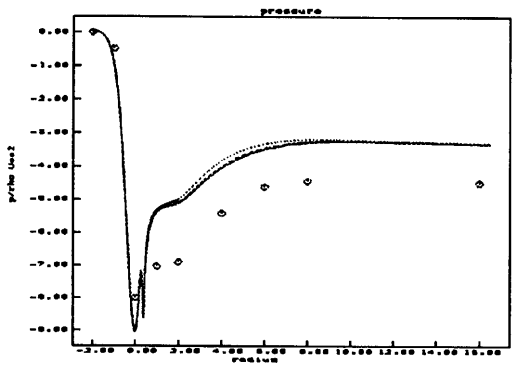

Figure 16. Axial profile of static pressure variation $p/\rho U_b^2$ along centreline for pipe constricton problem: symbols, experimental measurements; dotted lines, standard model; broken lines, modified model; full lines, non-linear model

generation that otherwise occurs with the standard model (the c_2 term does not contribute to the normal stresses).

A separate calculation was carried out with c_3 set to the default value of 0·26 instead of zero as with the calculations described above. This was done to investigate its influence on the isotropic turbulence generated (as this term only affects isotropic turbulence in axisymmetric flows). It was found that the results from the standard k–ε model were not changed significantly with the addition of the c_3 term.

Separate calculations were also carried out with the c_5 term. The default value gave levels of turbulence which were an order of magnitude higher upstream of the throat than those predicted even by the standard model. Positive values were less sensitive to the results, but even here erroneous turbulence was generated upstream of the throat. Consequently, $c_5 = 0$ is the correct value to use.

An investigation into the effect of the c_6 term was interesting. This term provides a mechanism for converting energy from the vorticity into (anisotropic) turbulence and this mechanism could well be responsible for the measured (anisotropic) turbulence levels downstream of the throat. However, no significant improvement in the results was found for any values of c_6. For negative values the prediction of pressure drop was actually worse. For a value of $c_6 = 0{\cdot}001$, only a very slight improvement occurred in the turbulence levels within the constriction, and for values larger than this, no further improvement was obtained.

5.2.5. Discussion. There are two distinct regions to consider, i.e. upstream and downstream of the throat. The experimental results presented indicate that the turbulence levels downstream of the throat are independent of the levels upstream and consequently the sources and sinks of turbulence dominate over convection and diffusion for this problem.

Agreement is poor downstream of the constriction for all the models considered, as shown in Figure 14, and both non-linear and modified models have only a minor impact on the flow predictions in this region. On the centreline the measured turbulence increases from near the throat downstream through the constriction, but all predictions fail to do this; the predicted turbulence levels are fairly constant on the centreline throughout the constriction. Possible explanations for this poor agreement downstream of the constriction are sought.

In the discussion about the effects of the c_6 term it was mentioned that when vorticity, which is generated at separation and resides in the core of the flow, is convected through the diffuser part of the constriction, significant turbulence could be generated. The experimental data show that the turbulence downstream of the throat is anisotropic, giving rise to axial and circumferential components of the normal stresses which are significantly larger than the component normal to the wall. This process could be modelled by the redistribution of energy from the mean flow shear stress (or vorticity) into the turbulence normal stresses. Both c_1 and c_6 terms are capable of exchanging energy between the rate of strain and normal stresses, but it has not proved possible to find a combination of these terms that provides the turbulence structure measured in the experiment.

Examination of the centreline bulk velocity within the constriction (Figure 15) shows that it is not predicted in accordance with the measurement. A possible explanation for the erroneously predicted turbulence distribution could be the poorly predicted velocity, i.e. perhaps a better prediction of flow separation would provide better agreement with the turbulence structure. It is judged, however, that this is not the main reason for the poor prediction.

It is possible that the standard k–ε model constants C_μ, $C_{1\varepsilon}$ and $C_{2\varepsilon}$ are not specified optimally for this problem and a respecification would improve the result quality.

A reason for the poor prediction of turbulence downstream of the constriction could be the availability of just one turbulent length scale within the turbulence model. At the constriction, turbulent eddies are stretched and this clearly provides more than one length scale, i.e. one parallel to

the flow direction and one normal to the flow direction, just as in the pipe expansion problem. The length scale predicted by k–ε models is the one mainly influenced by the wall distance, i.e. normal to the flow. A method of turbulence generation that is not included by the non-linear k–ε model is the cascade of the larger length scale, generated at the constriction by eddy stretching, to lower length scales with the consequential generation of turbulence. This mechanism cannot be reproduced by any one-length-scale turbulence model, including the non-linear k–ε model and Reynolds stress models.

The static pressure variation along the pipe wall is shown in Figure 16, the calculations by all turbulence models provide too much recovery within the constriction. This is due to the incorrect prediction of the position of separation, as the recovery provided by the flow until separation downstream of the throat is significant. The poor prediction of separation position could be due to an effect such as differences in wall roughness between calculation and experiment. The calculated flow could be made to separate at the position given by the experiment through the introduction of a trip in the mesh, which would significantly improve the prediction of pressure drop. However, it is unlikely that improvements in the prediction of turbulence would be enabled by this change.

In conclusion, the non-linear model with c_1 and c_2 specified as the default values unfortunately gives results which are significantly worse than those from the standard k–ε model. However, the non-linear model, with -1 times the default values for coefficients c_1 and c_2, and modified model both improve the prediction of turbulence upstream of the throat in comparison with the standard k–ε model. However, both these models are unable to improve the comparison of turbulence levels downstream of the throat, a region in which the sources and sinks of turbulence dominate over convection and diffusion. The two most likely reasons for the poor prediction are first the k–ε model constants used, which are not optimum for this flow, and secondly the presence of just one length scale.

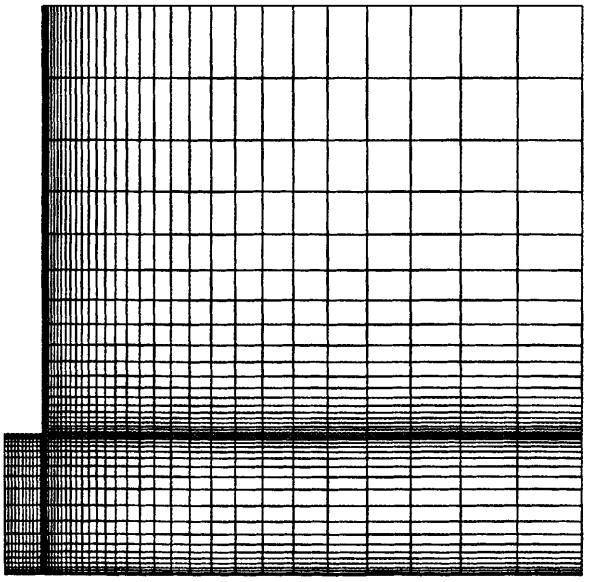

Figure 17. Finite element mesh used for impinging jet problem

5.3. Impinging jet problem

5.3.1. Description of problem and standard model results. This problem is described elsewhere;[3] the results presented here are for part A1. A fully developed pipe flow at a Reynolds number of 23,000, with a pipe diameter of 0·1016 m, exits the pipe and at two pipe diameters further downstream impinges on a flat plate. Figure 17 shows the mesh used for the problem.

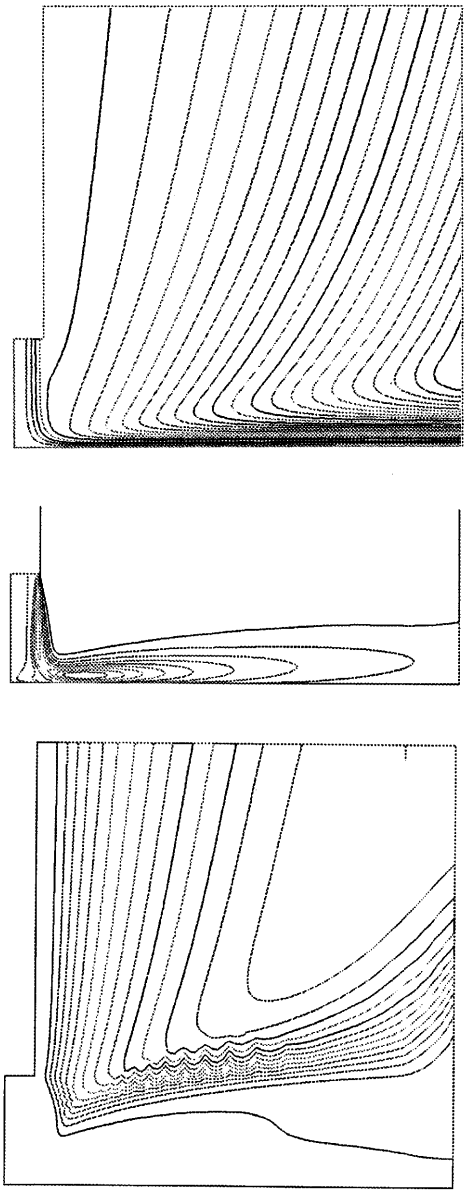

Figure 18. Contours of (from top) streamfunction, q and length scale for impinging jet problem

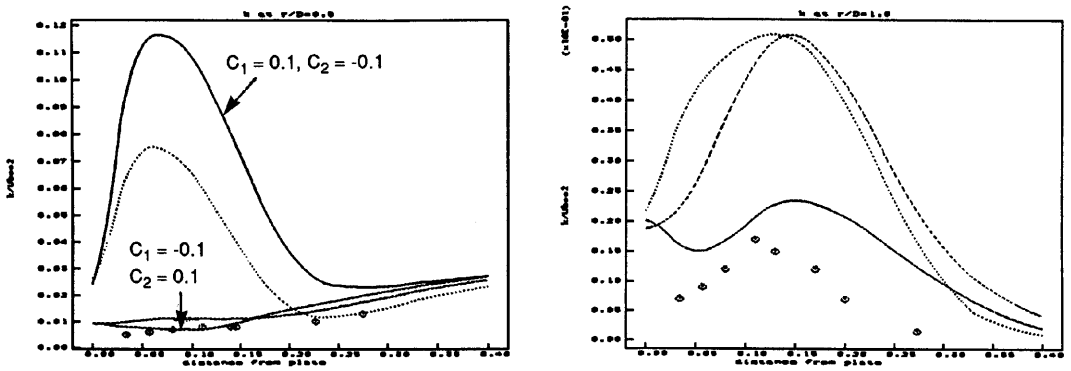

Figure 19. Axial profiles of k/U_b^2 at $r/D = 0{\cdot}5$ and $1{\cdot}0$: symbols, experimental measurements; dotted lines, standard model; broken lines, modified model; full lines, non-linear model

Figure 18 shows contours of streamfunction, turbulence speed q and turbulent length scale, the solution using the standard model. The standard k–ε model generates erroneous turbulence within the impingement region.

Figure 19 shows axial profiles of k within the impingement region of the jet, $r/D = 0{\cdot}5$ and $1{\cdot}0$ for all the models. The standard model overpredicts the turbulence within the impingement region by an order of magnitude. Figure 20 shows axial profiles of the axial and radial velocity components at $r/D = 0{\cdot}5$. Results from the extended models are described separately.

5.3.2. Modified model. The modified k–ε model predicts turbulence levels comparable with the experimental data within the central impingement region, as shown in Figure 19. At the edge of the impingement region, however, the turbulence prediction is around a factor of four too high, which is no better than the standard model. The prediction of the velocity is similar with all models, as shown in Figure 20.

5.3.3. Non-linear model. Two cases were considered, one with the default values of c_1 and c_2 and one with values $-1{\cdot}0$ times the default values. All the other coefficients were set to zero.

With $c_1 = -0{\cdot}1$ and $c_2 = 0{\cdot}1$, Figure 19 shows that turbulence levels are comparable with experiment within the central impingement region, i.e. erroneous turbulence is not generated within

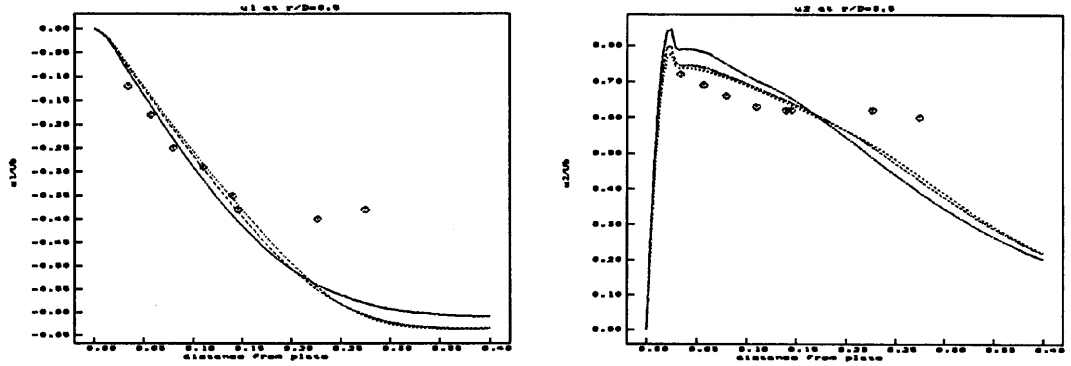

Figure 20. Axial profiles of u_1/U_b and at u_2/U_b at $r/D = 0{\cdot}5$: symbols, experimental measurements; dotted lines, standard model; broken lines, modified model; full lines, non-linear model

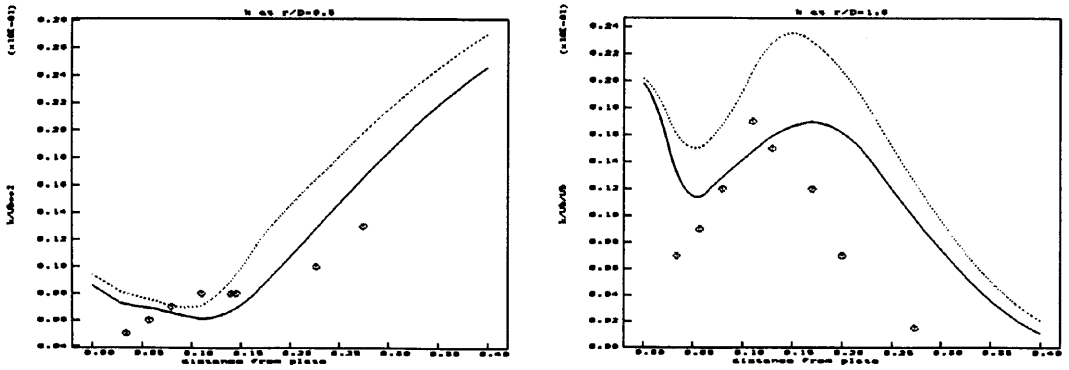

Figure 21. Axial profiles of k/U_b^2 at $r/D = 0{\cdot}05$ and $1{\cdot}0$: symbols, experimental measurements; dotted lines, non-linear model with $c_6 = 0$; full lines, non-linear model with $c_6 = 0{\cdot}001$

the whole impingement region, unlike from the standard model. The results in this region are comparable with those from the modified model. However, at the edge of the impingement region, turbulence levels are only slightly overpredicted by the non-linear model, whereas the modified model results are no better than those of the standard model. Consequently, the performance of the non-linear model for this problem is significantly better than that of the modified k– ε model, using the default values of the coefficients c_1 and c_2.

With c_1 and c_2 set to -1 times their default values, Figure 19 shows that agreement of turbulence energy with experiment is significantly worse than that obtained from the standard k–ε model, i.e. even more erroneous turbulence is generated within the impingement region.

The results are generally sensitive to values of c_5 and c_6. All non-zero values of c_5 provide solutions that are significantly worse than those presented; hence $c_5 = 0$ is the best value to take. A value of $c_6 = 0{\cdot}001$ in conjunction with the default values of c_1 and c_2 does, however, provide a solution that is an improvement over the results presented within the impingement region. Figure 21 shows a comparison between profiles of k at $r/D = 0{\cdot}5$ and $1{\cdot}0$ with this value of c_6, with $c_6 = 0$ and the measurements. Although the turbulence predictions are better, the spreading rate of the jet is still incorrectly predicted. For values of c_6 greater than $0{\cdot}001$ the solution quality deteriorates.

5.3.4. Discussion. The velocity profiles in Figure 20 show that the jet spreads along the wall at a different rate from the prediction for all the models; this is in line with predictions for both pipe expansion and pipe constriction problems.

A non-linear model using the default values of c_1 and c_2 and a small value of $c_6 = 0{\cdot}001$ gives the best results from the pipe constriction problem, for which values of c_1 and c_2 needed to be set to -1 times the default values before the best results could be achieved.

6. DISCUSSION

A similar validation exercise to that described above should also be carried out for the RNG (renormalization group) version of the k–ε model. A widely quoted improvement in results attributed to the RNG model, in comparison with the standard k–ε model, is that of the prediction of eddy lengths. However, there are much more important engineering comparisons to be made, such as turbulence fields and pressure drop, and indeed the 'correct' prediction of an eddy length proves nothing about the quality of results. For example, examination of a photograph[11] of a jet exiting a

round pipe at a Reynolds number of 30,000 clearly shows that the jet retains its low-turbulence structure for some distance after exiting the pipe, before breaking down into larger-length-scale turbulence. Any k–ε model predicts turbulence instantaneously at the pipe exit, owing to the fact that the differential equations contain a singularity there, and hence the breakdown into turbulence necessarily starts upstream from reality. If the primary eddy length predicted by the turbulence model is in agreement with the experiment for this case, then clearly the spreading rate of the shear layer has been incorrectly predicted by the turbulence model, in spite of appearances. Hence the quality of results from the RNG model also requires thorough investigation. This is left for others to consider.

The results presented in this paper have shown that an improvement in results from the k–ε model could possibly be obtained by a retuning of the model constants C_μ, $C_{1\varepsilon}$ and $C_{2\varepsilon}$. For example, the spreading rate of shear layers needs improving. Since the model was tuned a long time ago and there is significantly more experimental information available now, retuning of the model constants is a sensible option. The original model constants were derived from the results of three flows: turbulence decay behind a grid, turbulence provided by a shear layer and turbulence provided by a log layer. However, the fitting to a log layer is not correct. Three different types of flow problem should be chosen against which the model constants can be fitted. The problem of turbulence decay behind a grid is a flow that analytically provides an expression for one of the constants in terms of the other two. The other two flows chosen should be one in which sources and sinks dominate over convection and diffusion and the other in which convection and diffusion are significant. The pipe contraction problem is a possibility for the former flow, concentrating on the behaviour downstream of the throat, and the pipe expansion a possibility for the latter flow, as the experimental results are such good quality. Any simulation of the pipe contraction problem should ensure that flow separation occurs at the right position by, for example, providing a trip in the model at the experimental separation location.

As with all current turbulence models, only one turbulent length scale is provided by the k–ε models. Consequently, for problems in which there is clearly more than one length scale involved, such as those for which turbulent eddies are stretched, the quality of prediction will remain limited. There is plenty of room for development in this area of turbulence modelling, however. For example, it is possible to calculate an anisotropic length scale based on the velocity correlations $\overline{(u_i' u_j')}$ and another variable such as turbulence frequency f (or ω, as in the currently fashionable k–ω model). This is a much better variable to use than ε, since frequency is isotropic even if the dissipation rate (ε) or length scale is not. This formulation will provide an anisotropic length scale if the velocity correlations are anisotropic. Again, this is left for others to consider.

7. CONCLUSIONS

1. Both modified and non-linear k–ε models have been successfully implemented in FEAT. Solutions are obtained for a cost that is similar to that of a standard model solution.

2. In 2D the anisotropic behaviour of the non-linear k– ε model is dependent on the terms involving c_5 and c_6 only. Hence c_1, c_2, c_3 and c_4 can be set to zero for 2D problems.

3. The following statements are generally true for all non-swirling axisymmetric flows using the non-linear model.

(a) The c_2 term does not contribute to the normal stresses and therefore does not provide a mechanism for anisotropy of the turbulence. The term does, however, provide a contribution to the shear stress.

(b) The term involving c_3 generates only isotropic turbulence, i.e. $\overline{(u_1' u_1')} = \overline{(u_2' u_2')}$ and $\overline{(u_1' u_2')} = 0$. This is not the objective of a non-linear k–ε model, and although it does affect the isotropic

turbulence, it was found to have only a small effect on the problems considered. Hence c_3 is set to zero.

(c) The term involving c_4 makes no direct contribution to turbulence generation, although the velocity is affected by the term. This may in turn affect the turbulence, but for the problems considered, no improvement was found using the term. Consequently, c_4 is set to zero.

Three validation axisymmetric problems—flow through a pipe expansion, flow through a pipe constriction and an impinging jet problem—were used to test the two turbulence models. The next three conclusions were found from examination of the non-linear model using the validation problems.

4. The term involving c_5 has not produced results that are an improvement in comparison with those involving just the c_1 and c_2 terms. Consequently, c_5 is set to zero.

5. Only a small value of $c_6 = 0{\cdot}001$ provided solutions that were an improvement over the model which included just c_1 and c_2 terms; a significant improvement was found only for the impinging jet problem.

6. The setting of c_3, c_4, c_5 and c_6 is not in agreement with the proposed default values in Reference 8. The values chosen were those that gave the best fit to experimental measurements for the three validation problems.

7. For the problem involving flow through a pipe constriction, values of $c_1 = 0{\cdot}1$ and $c_2 = -0{\cdot}1$ gave the best agreement with measurements. With $c_1 = -0{\cdot}1$ and $c_2 = 0{\cdot}1$ (the proposed default values[8]) the results are significantly worse than those from the standard k–ε model. For the impinging jet problem, values of $c_1 = -0{\cdot}1$ and $c_2 = 0{\cdot}1$ gave the best agreement with measurements; specifying $c_1 = 0{\cdot}1$ and $c_2 = -0{\cdot}1$ gave significantly worse results in comparison with the standard k–ε results. These two sets of results are in direct contradiction with each other.

8. The non-linear and modified models produce almost identical solutions to the standard k–ε model for the pipe expansion problem and no advantage is gained by using the extended models. All the solutions give acceptable agreement for the gross features in the flow when compared with the measurements, apart from within the recirculation region, where turbulence levels are significantly underpredicted, and near the centreline edge of the shear layer, owing to the poor prediction of the spreading rate of the shear layer.

9. The non-linear and modified models give a significantly better prediction of turbulence distribution than does the standard k–ε model upstream of the throat for the problem of flow through a pipe constriction. Downstream of the throat, however, which is a region in which the sources and sinks of turbulence dominate over convection and diffusion, the prediction is no better. The reason for the discrepancies with experiment is the incorrect prediction of the shear layer spreading rate.

10. For the impinging jet problem a significantly better prediction of turbulence levels is obtained using the non-linear k–ε model rather than the standard k–ε model, as erroneous turbulence is not generated within the impingement region. The quality of solution of the non-linear model is also significantly better than the modified model solution, which itself gives a significant improvement in turbulence prediction within the impingement region. Nevertheless, the spreading rate of the jet is poorly predicted by all the turbulence models.

11. To improve the prediction of the spreading rate of shear layers by two-equation turbulence models, for example, we propose that a retuning of the three model constants in the k–ε model be undertaken, using experimental results from the pipe expansion and pipe contraction problems, also including the problem of turbulence decay behind a grid.

12. The experimental results available for the pipe expansion problem clearly show the presence of more than one length scale. We propose an investigation into the modelling of anisotropy in turbulent length scale, which may improve the prediction of turbulence structure in flows.

REFERENCES

1. R. T. Szczepura, 'Flow characteristics of an axisymmetric sudden pipe expansion: results obtained from the turbulence studies rig. Part 1, Mean and turbulence velocity results', *CEGB Rep. TRPD/B/0702/N85*, 1985.
2. M. D. Deshpande and D. P. Giddens, 'Turbulence measurements in a constricted tube', *J. Fluid Mech.*, **97**, 65–89 (1980).
3. J. F. Brison and G. Brun. *15th Meeting of the IAHR/ERCOFTAC Working Group on Refined Flow Modelling*; *Round Normally Impinging Turbulent Jets*, Laboratoire de Mecanique des Fluides et d'Acoustique, Ecole Centrale de Lyon, 1991.
4. *FEAT Version 2.3.5 User Guide*, Nuclear Electric, Gloucester, 1994.
5. S. Hickmott, 'Computational fluid dynamics—an analysis of cost versus accuracy', *CEGB Rep. RD/B/6013/R88*, 1988.
6. R. M. Smith, 'A practical method of two-equation turbulence modelling using finite elements', *Int. j. numer. methods fluids*, **4**, 321–336 (1984).
7. C. G. Speziale, 'On nonlinear *K–l* and *K–ε* models of turbulence', *J. Fluid Mech.*, **178**, 459–475 (1987).
8. T. J. Craft, B. E. Launder and K. Suga, 'Extending the applicability of eddy viscosity models through the use of deformation invariants and non-linear elements', in *Refined Flow Modelling and Turbulence Measurements*, Presses Ponts et Chaussees, Paris, 1993, pp. 125–132.
9. A. G. Hutton and R. T. Szczepura, 'Turbulent flow and heat transfer in a sudden pipe expansion: a comparison of current models of turbulence', *CEGB Rep. TPRD/B/0926/R87*, 1987.
10. R. T. Szczepura, 'Flow characteristics of an axisymmetric sudden pipe expansion: results obtained from the turbulence studies rig. Part 2: Spectral measurements', *GECB Rep. TPRD/B/0703/R86*, 1985.
11. M. Van Dyke, *An Album of Fluid Motion*, Parabolic, Stanford, 1982, Caption 117.

